Tunable optical fiber devices based on broadband long-period gratings and pumped microfluidics

Bharat R. Acharya and Tom Krupenkin
Bell Laboratories, Lucent Technologies, Murray Hill, New Jersey 07974

Siddharth Ramachandran and Z. Wang
OFS Laboratories, Murray Hill, New Jersey 07974

C. C. Huang
School of Physics and Astronomy, University of Minnesota, Minneapolis, Minnesota

John A. Rogers[a)]
Department of Materials Science and Engineering and Department of Chemistry, Beckman Institute and Seitz Materials Research Laboratory, University of Illinois, Urbana-Champaign, Illinois 61801

(Received 19 June 2003; accepted 8 October 2003)

This letter describes classes of tunable microfluidic fiber (μFF) devices that use specially designed long-period gratings in which the phase matching condition is satisfied over a wide spectral range. Dynamic tuning is achieved by electrowetting-based pumping of microfluidic plugs back and forth over the gratings. As specific examples, we demonstrate dynamically tunable broadband attenuators and filters with adjustable profiles by using fluids with different refractive indices. These devices have attractive features that include in-fiber design and polarization-independent behavior together with low-power, nonmechanical, fully reversible, and latchable tuning. © *2003 American Institute of Physics.* [DOI: 10.1063/1.1633331]

Tunable optical fiber devices are emerging as valuable components of high-speed optical communications systems. Long period gratings (LPGs), which couple the fundamental core mode to higher order copropagating cladding modes, have been studied extensively because of their potential applications in band rejection,[1] and gain control.[2] We recently demonstrated that microfluidics actuated by electrowetting effects provides a convenient means to tune the optical properties of these and other fiber structures.[3,4] These microfluidic fiber (μFF) devices offer low power operation and a rich range of tuning mechanisms. A drawback of μFF devices that use conventional LPGs, however, is that the tuning range is typically only a few nanometers, primarily limited by the bandwidth of the LPGs. Although LPGs based on large index variations, induced by microbending of fiber, yield relatively large bandwidth (~30 nm for 20 dB mode conversion)[5] they suffer from polarization dependent characteristics, and high insertion losses (~0.4 dB). Recently, we showed that with specially engineered few-mode fiber it is possible to achieve a turn around point (TAP) in the LPG phase matching condition, which yields a wide bandwidth (20 dB coupling over 63 nm), low loss, and polarization independent performance with only modest index variations.[6] In this letter, we combine μFF designs and TAP LPGs to build a class of fiber device that provides continuously tunable attenuation and spectral reshaping over a large bandwidth. The transmission characteristics of these μFF devices are controlled by pumping fluids with different refractive indices around the TAP LPG by use of electrowetting pumps and planar microfluidic networks. These devices have low power, latchable operation with polarization independent and low loss behavior over a wide wavelength range.

In LPGs, the spectral dependence of the resonant coupling is primarily determined by the difference in the effective indices between the two coupling modes (Δn) and the difference in their corresponding group indices (Δn_g) and is given by:[6]

$$\frac{d\Lambda}{d\lambda_{\mathrm{res}}} = \frac{\Delta n_g}{\Delta n^2},$$

where λ_{res} is the resonant wavelength and Λ is the grating period. Conventional LPGs exhibit strong mode conversion at a specific resonant wavelength, with near-monotonic decrease in coupling over bandwidths of 3–5 nm. If a fiber is designed such that one of the higher order cladding modes transitions, as a function of wavelength, from being localized primarily in the fiber cladding to a spatial profile involving significant overlap with the surroundings, a unique feature results in the phase matching curve (plot of grating period versus wavelength). This mode transition leads to matching of the group indices of the fundamental and the higher order cladding mode, which in turn makes $\Delta n_g = 0$, thus leading to a maxima (called TAP, henceforth) in the phase matching curve. The resulting spectrum has a wide bandwidth and is extremely sensitive to the optical properties of the surroundings. The extreme sensitivity has, for example, recently demonstrated[7] to yield more than 25 dB amplitude modulations with external index modulations of only 10^{-4}.

Figure 1(a) shows simulated phase matching curves for a LPG, with a period of 150 μm and UV induced refractive index gradient $\Delta n = 1.54 \times 10^{-3}$, in a fiber engineered to possess a TAP in ambient refractive index $n = 1.39$ at 1530 nm. The figure also depicts the phase matching curves for the same grating in surroundings with different refractive indices ($n = 1.33$ and $n = 1.41$). When the index is higher than 1.39, the phase matching condition is satisfied at two different wavelengths [indicated by arrows in Fig. 1(a)] splitting the

a)Electronic mail: jrogers@uiuc.edu

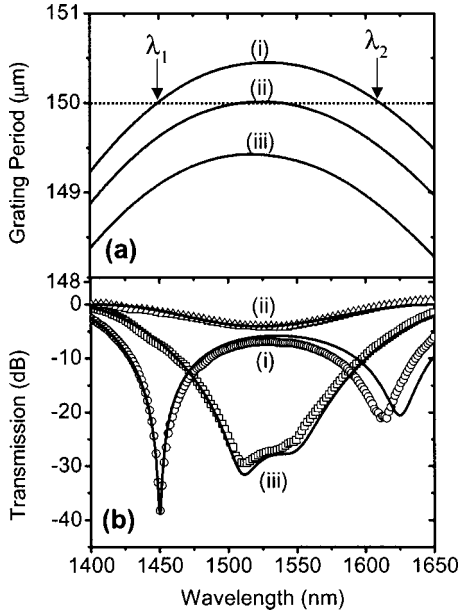

FIG. 1. (a) Simulated phase matching curves for a LPG that couples the fundamental core mode to the $LP0_{12}$ cladding mode immersed in fluids with different refractive indices (i) $n=1.41$, (ii) $n=1.39$, and (iii) $n=1.33$. For a grating with 150 μm period, the phase matching curves show resonance at two wavelengths (indicated by vertical arrows), turn around point (TAP), and no resonance for (i), (ii), and (iii), respectively. (b) corresponding simulated (solid curves) transmission spectra for the three fluids in (a). The symbols show the experimental transmission spectra for a grating with 150 μm period optimized to exhibit TAP in silicone oil ($n=1.39$). (△), (□), and (○) correspond to the case when the grating is immersed in water ($n=1.33$), silicone oil, and 41% sodium dichromate solution ($n=1.41$), respectively.

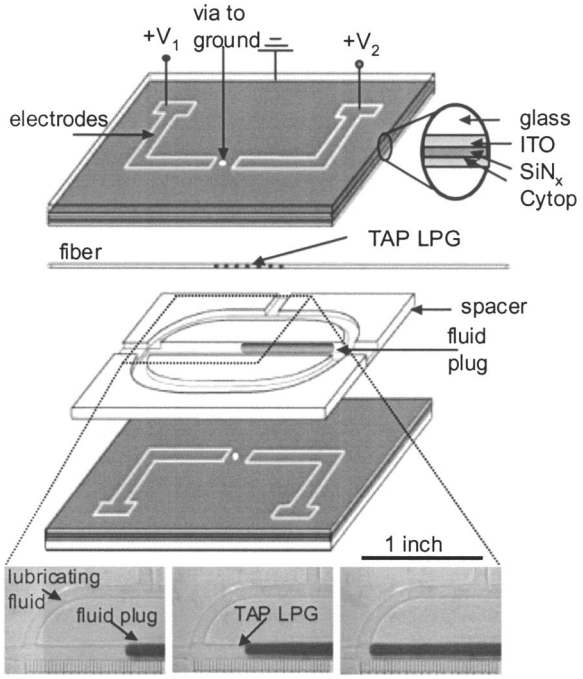

FIG. 2. Schematic exploded view of the microfluidic system and electrowetting pumps. The white lines on the top and bottom electrode substrates separate the electrodes from the rest of the substrate, which is electrically grounded. By swapping V_1 and V_2 between zero and positive potentials the conductive fluid can be pumped into and out of overlap with the fiber grating. The inset shows three snapshots of the section of the μFF device as the conducting fluid advances over the TAP grating.

spectrum into two LPG-like resonance features. When the index is lower than 1.39, the phase matching condition is no longer satisfied at any wavelength and, as a result, there is diminished coupling between the core mode and the co-propagating cladding modes. The solid lines in Fig. 1(b) show the corresponding simulated transmission spectra. For experimental demonstration of this effect, we used gratings written into specially designed optical fibers that support the fundamental core mode and the $LP0_{12}$ cladding mode such that a grating period of 150 μm couples these two modes at a wavelength of ~1530 nm. The thickness of the cladding is then reduced by etching in hydrofluoric acid so that the $LP0_{12}$ mode makes a transition from the cladding to the surroundings above this wavelength when the grating is fully covered with silicone oil (polydimethylsiloxane, DMS-T02, Gelest, Inc, $n=1.39$), i.e., a TAP is achieved in the phase matching curve at this wavelength in silicone oil. The curves depicted by symbols in Fig. 1(b) show the spectra when the grating is immersed in three different fluids: silicone oil, water ($n=1.33$) and 41% aqueous solution of sodium dichromate ($n=1.41$). As predicted by the simulation, the grating optimized for TAP in silicon oil shows splitting (broadband attenuation) when immersed in fluid with higher (lower) refractive index than that of silicon oil. We note that the resonance feature does not completely disappear even when the TAP grating is fully immersed in water and shows an ~3 dB insertion loss. This loss is associated with the fact that the refractive index of water is slightly higher than that is needed for the grating optimized for TAP in silicone oil. An optimized refractive index combination of two fluids shows a near perfect disappearance of the resonance feature.[7] Thus, by covering the grating structure with fluids with different refractive indices, it is possible to switch the optical transmission characteristics of the grating between the TAP splitting and TAP-attenuation states. We exploit these TAP LPG effects with an integrated microfluidic network and electrowetting pumps to form a μFF device that offers a variety of broadband, continuously tunable optical characteristics.

Figure 2 shows a schematic view of the three components of the microfluidic part of the device: an insulating spacer that has micromachined channels for confining the motion of the fluids and two glass substrates with patterned indium tin oxide (ITO) electrodes that provide the electrowetting pumps. The spacer consists of a 2 mm thick sheet of poly(methyl methacrylate) (PMMA) micromachined to confine the motion of the fluids in a recirculating geometry that minimizes back pressure during pumping. A straight section that bisects the oval racetrack houses the fiber grating. Motion of a conducting fluid plug (either water with a small amount of ionic salt: 1-ethyl-3-methyl-1H-imidazolium trifluoromethanesulfonate or 41% aqueous solution of sodium dichromate) in this straight section is assisted by the lubricating layer of the silicone oil[8] that fills the rest of the channels. Unlike the previous designs,[3] which used electrodes on only one substrate, we use electrodes on both substrates to provide improved electrowetting pumping. The other components and detailed operation of the device are similar to those described elsewhere.[4] When the ITO electrodes are at different potential than the conductive plug, then the electrowetting effect leads to different contact angles at two ends of the plug. The resulting force imbalance causes the plug to move toward the electrode that is at higher potential.

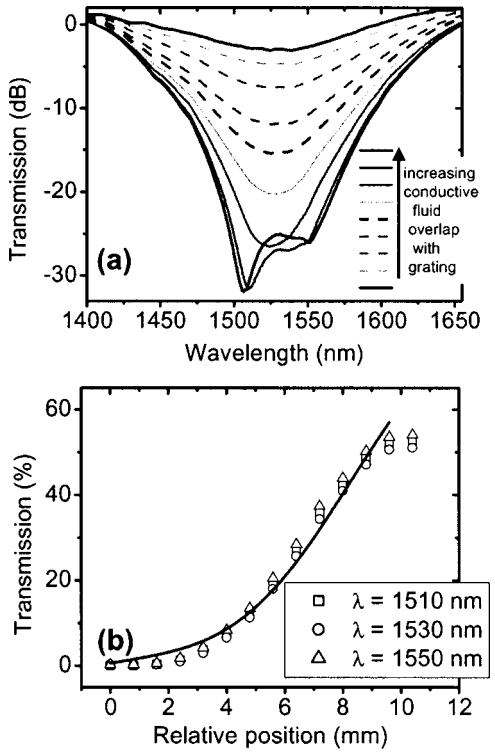

FIG. 3. (a) Evolution of the transmission spectrum as the conductive plug (water with ionic salt) advances over the LPG optimized for TAP in silicon oil. As the conductive fluid overlaps gradually over grating structure, the resonance feature disappears. (b) The variation of the transmitted intensity as a function of relative position of the conductive fluid over the grating structure for different wavelengths. The solid lines are the theoretical fits to the experimental data using Eq. (1) with $\kappa=0.1538$, $\delta_1=0$, and $\delta_2=0.13791$.

Figure 3(a) shows the evolution of the optical transmission characteristics of the TAP LPG as the lower index conducting fluid (i.e., water with ionic salt) is pumped into overlap with the grating structure. The results illustrate continuous fluidic-based tuning between the two states expected based on the results in Fig. 1. Figure 3(b) shows the variation of the optical transmission of this broadband attenuator as a function of the relative position of the silicone oil–water interface for three different wavelengths centered around 1530 nm. The result is a variable 20 dB attenuation feature that extends over more than 40 nm. In order to understand these results quantitatively, we consider the grating partially covered by two fluids as comprising two decoupled states (fiber covered with silicone oil and fiber covered with conductive fluid). We expect this approximation to be valid due to the sharp contrast in the refractive indices at the fluid interface. In this case, the resultant coupling strength is a linear superposition of two separate gratings with corresponding strengths. Then the intensity, I, can be written as:

$$I=1-\kappa^2\frac{\sin^2[\sqrt{(\kappa l)^2+(\delta_1 l)^2}]}{\kappa^2+\delta_1^2}-\kappa^2\frac{\sin^2[\sqrt{(\kappa[L-l])^2+(\delta_2[L-l])^2}]}{\kappa^2+\delta_2^2}, \quad (1)$$

where L is the total length of the grating, κ is its coupling coefficient (proportional to the induced index change), l is the length, and δ_1 is the detuning associated with the part of the grating immersed in one of the fluids, while δ_2 is the detuning associated with the grating immersed in the other fluid. The detuning coefficient δ is defined as $\delta=2\pi/\Lambda-(\beta_1-\beta_2)$ with Λ being the grating period and β_1 and β_2 being the respective propagation constants of the fundamental core mode and the $LP0_{12}$ core mode. The solid line represents the theoretical fit to the experimental data using Eq. (1). This simple model yields reasonably good agreement with the experimental results.

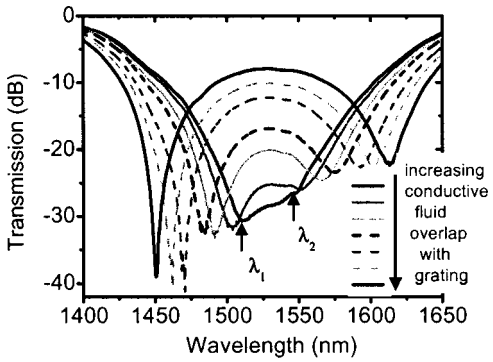

FIG. 4. Evolution of the transmission spectrum as the conductive plug (41% aqueous solution of sodium dichromate) advances over the same grating as in Fig. 3. As the conductive fluid overlaps gradually over grating structure, the resonance feature splits in to two LPG-like features.

For another demonstration of a TAP LPG-based μFF device, we used the chromate solution, which has higher refractive index than that of silicone oil, as the conducting plug to induce and tune a split spectrum using the same TAP grating. Figure 4 shows the spectrum splitting into two separate features as the degree of overlap increases. The spacing between the resonant wavelengths i.e., the separation between the two wavelengths indicated by arrows in Fig. 4 increases with increase in the overlap of the fluid over the grating. A system with higher refractive index will produce sharp resonance features, each of which can potentially be used as a narrow band filters.

This concept can be extended to multiple fluids with different refractive indices for dynamically switchable attenuation, splitting, and superstructures, etc. These and related μFF devices have numerous potential applications in optical communication system.

This research was supported in part by the NSF GOALI Grant.

[1] A. M. Vengsarkar, P. J. Lemaire, J. B. Judkins, V. Bhatia, T. Erdogan, and J. E. Sipe, J. Lightwave Technol. **14**, 58 (1996).
[2] H. Lebidi, J.-J. Guerin, V. Girardon, X. Bonnet, C. Simonneau, R. Boucenna, C. D. Barros, N. Dely, and I. Riant, Conference Proceedings European Conference on Optical Communication, PD1.8 (2002).
[3] J. Hsieh, P. Mach, F. Cattaneo, S. Yang, T. Krupenkin, K. Baldwin, and J. A. Rogers, IEEE Photonics Technol. Lett. **15**, 81 (2003).
[4] P. Mach, T. Krupenkin, S. Yang, and J. A. Rogers, Appl. Phys. Lett. **81**, 202 (2002).
[5] C. D. Poole, H. M. Presby, and J. M. Meester, Electron. Lett. **30**, 1437 (1994).
[6] S. Ramachandran, Z. Wang, and M. Yan, Opt. Lett. **27**, 698 (2002).
[7] Z. Wang, A. Hale, and S. Ramachandran, Proceedings Conference Lasers and Electro-Optics, Ctul4 (2003).
[8] T. Krupenkin, S. Yang, and P. Mach, Appl. Phys. Lett. **82**, 316 (2003).